



The elongation factor 1-alpha as storage reserve and environmental sensor in *Nicotiana tabacum* L. seeds

Emma Cocco^{a,b}, Domenica Farci^{a,c,*}, Giulia Guadalupi^d, Barbara Manconi^d, Andrea Maxia^b, Dario Piano^{a,**}

^a Laboratory of Plant Physiology and Photobiology, Department of Life and Environmental Sciences, University of Cagliari, Viale S. Ignazio da Laconi 13, Cagliari 09123, Italy

^b Laboratory of Economic and Pharmaceutical Botany, Department of Life and Environmental Sciences, University of Cagliari, Viale S. Ignazio da Laconi 13, Cagliari 09123, Italy

^c Department of Plant Physiology, Warsaw University of Life Sciences – SGGW, Nowoursynowska Str.159, Warsaw 02-776, Poland

^d Department of Life and Environmental Sciences, University of Cagliari, Cagliari 09124, Italy

ARTICLE INFO

Keywords:

Nicotiana tabacum
Seeds
Soluble proteins
Protein stability
Mass spectrometry

ABSTRACT

Given their critical role in plant reproduction and survival, seeds demand meticulous regulatory mechanisms to effectively store and mobilize reserves. Within seeds, the condition of storage reserves heavily depends on environmental stimuli and hormonal activation. Unlike non-protein reserves that commonly employ dedicated regulatory proteins for signaling, proteinaceous reserves may show a unique form of 'self-regulation', amplifying efficiency and precision in this process. Proteins rely on stability to carry out their functions. However, in specific physiological contexts, particularly in seed germination, protein instability becomes essential, fulfilling roles from signaling to regulation. In this study, the elongation factor 1-alpha has been identified as a main proteinaceous reserve in *Nicotiana tabacum* L. seeds and showed peculiar changes in stability based on tested chemical and physical conditions. A detailed biochemical analysis followed these steps to enhance our understanding of these protein attributes. The protein varied its behavior under different conditions of pH, temperature, and salt concentration, exhibiting shifts within physiological ranges. Notably, distinct solubility transitions were observed, with the elongation factor 1-alpha becoming insoluble upon reaching specific thresholds determined by the tested chemical and physical conditions. The findings are discussed within the context of seed signaling in response to environmental conditions during the key transitions of dormancy and germination.

1. Introduction

The role of protein instability and degradation in cell signaling has been widely investigated and observed across diverse contexts at all levels of life (Adam, 1996; Faden et al., 2019; Jurkiewicz and Batoko, 2018). This holds true for seeds and their regulation of reserves in terms of both accumulation and mobilization. Various areas of cell biology provide examples of signaling mechanisms influenced by protein instability. Spanning from gene regulation and expression to epigenetics, the described phenomena encompass not only indirect effects at the gene level but also include direct interactions between proteins (Villalobos Solis et al., 2020; Zientara-Rytter and Sirko, 2016). Among

these direct mechanisms, the most prevalent ones involve protein-mediated modulation of key enzymes in the context of metabolic regulation, as well as protein-mediated activities that can influence membrane permeability and trafficking (Jin et al., 2018; Ling et al., 2019). In this respect, seeds present a fascinating example where this regulation needs to be meticulously orchestrated, aligning with the plant's cycle during fruit and seed maturation, and subsequently during seed germination. In both instances, these processes are steered by hormonal signals originating from the embryo (Ali et al., 2020; Antoni et al., 2011; Holman et al., 2009), leading to either the accumulation or mobilization of reserves. Among seeds, those with proteinaceous reserves stand out as particularly interesting. Here, the regulation and

* Corresponding author at: Laboratory of Plant Physiology and Photobiology, Department of Life and Environmental Sciences, University of Cagliari, Viale S. Ignazio da Laconi 13, Cagliari 09123, Italy.

** Corresponding author.

E-mail addresses: domenica.farci@unica.it (D. Farci), dario.piano@unica.it (D. Piano).

<https://doi.org/10.1016/j.plantsci.2024.112113>

Received 25 November 2023; Received in revised form 30 March 2024; Accepted 6 May 2024

Available online 8 May 2024

0168-9452/© 2024 The Author(s). Published by Elsevier B.V. This is an open access article under the CC BY-NC-ND license (<http://creativecommons.org/licenses/by-nc-nd/4.0/>).

sensing of reserves are anticipated to primarily involve self-regulatory mechanisms through direct sensing, eliminating the necessity for protein effectors to mediate the signal (Dorone et al., 2021; Field et al., 2023; Piskurewicz et al., 2023). In the model plant *Nicotiana tabacum* L., the reserves within the seeds consist primarily of proteins and oils (Li et al., 2018). In this model organism, the intricate mechanisms governing seed dormancy, activation, and their responsiveness to environmental factors and hormones have been extensively documented (Agacka-Moldoch et al., 2021; Farci et al., 2020; Li et al., 2016; Cocco et al., 2022). In alignment with these studies, the current research focuses on the soluble protein fraction of tobacco seeds, which represents a major component. This fraction was notably enriched in a dominant protein pool, characterized as a complex with high molecular weight. This complex has been identified through Mass Spectrometry (MS) as the elongation factor 1- α (EF1- α), a highly conserved protein. In plants, EF1- α plays a crucial role in regulating protein synthesis and is involved in responses to abiotic stressors such as temperature, salt, and drought. Additionally, it also contributes to environmental adaptation (Fu et al., 2012; Xu et al., 2023). Accordingly, this specific fraction was employed as a tool to explore the seed's reaction to various chemical and physical factors, including temperature, pH, and salt concentrations. The isolated complex was identified as the predominant protein in the seeds, underscoring its paramount role in the protein reserves of this particular species. When subjected to a range of temperature gradients, shifts in pH, and variations in salt concentration, the enriched extract and its primary component, the EF1- α complex, show distinct behaviors. More precisely, under these circumstances, the protein undergoes systematic transitions characterized by alterations in solubility. These transitions are analyzed as unique attributes that could potentially facilitate the evaluation of environmental factors like temperature, water availability, and nutrient levels. These properties could serve as an effective tool for gathering information about the prevailing environmental conditions in relation to the seed's physiological stage. The EF1- α is a multifaceted protein, known for its crucial role in protein translation, directly influencing ribosomal activity, as well as its transcription and post-transcriptional regulation in response to salt stress, fluctuations in Ca^{2+} , and shifts in pH (Ransom-Hodgkins et al., 2000; Kuang et al., 2019). Moreover, previous studies evidenced its positive correlation with the Lys-rich reserve proteins in maize embryo and reported the EF1- α as an indicator of protein quality, specifically in cereal crops and corn lines (Lopez-Valenzuela et al., 2004; Sun et al., 1997). This study provides evidence for its designation as a primary seed reserve, capable of engaging in self-regulatory mechanisms through the direct sensing of environmental factors. Results are discussed in the context of seeds germination/dormancy where effective and precise environmental stimuli must be finely interpreted for their reliability.

2. Materials and methods

2.1. Plant material and protein extraction

Nicotiana tabacum L. (cv. *Petit Havana*) seeds were obtained from plants grown at 25°C, 50% relative humidity, and a photoperiod of 12 h of light per day. As a light source a LED lamp with a light intensity of 150–200 $\mu\text{mol photons}/(\text{s}\cdot\text{m}^2)$ has been used. For protein extraction, seeds were added with 400 μL of Grinding Buffer (GB; 50 mM MES pH 6.5; 10 mM $\text{MgCl}_2\cdot 6\text{H}_2\text{O}$; 10 mM $\text{CaCl}_2\cdot 2\text{H}_2\text{O}$) and mechanically ground with a pestle for micro-centrifuge tube. After fragmentation and homogenization, the suspension of broken seeds was centrifuged at 15000 $\times g$ for 10 min at room temperature to remove the seeds' fragments. After collecting the supernatant, the pellet underwent a further extraction step in 100 μL GB. This extraction procedure was always performed with three parallel and independent preparations starting from 40 mg seed each. Immediately after preparation, the obtained samples were stored at -20°C and used for the subsequent steps of analysis. Preliminary experiments adding protease inhibitors to the GB

did not lead to any difference in terms of protein patterns, therefore the final protocol has been designed without. Unless differently stated, the entire procedure has been performed at room temperature.

2.2. Size exclusion chromatography

The obtained protein extraction pool was subjected to Size Exclusion Chromatography (SEC) either using a Superdex 200 10/300 GL (S200) or a Superdex Increase 75 10/300 GL (S75) columns (Cytiva Life Sciences) previously equilibrated in GB. The S200 run was carried out at a flow rate of 0.8 mL/min on 200 μL of injected volume and monitored by measuring the absorbance at 254 nm and 280 nm. The S75 run was performed at 0.5 mL/min and recorded at the absorbance of 280 nm. To ensure that the presence of small molecules did not alter the chromatographic profile, the S75 run was also performed in the same experimental condition with a sample where the small components were removed by using a 10 kDa MW cutoff concentrator. The elution volume for each peak were used for calculating the apparent mass of the peaks in the sample. Apparent masses were calculated with respect to a regression curve obtained by plotting the logarithm of the masses of a molecular marker (Gel Filtration Standard, Biorad) with respect to their elution volume, as shown by Haniewicz and coworkers (Haniewicz et al., 2015). In these studies, all chromatography columns were subjected to the ReGenFix procedure (<https://www.regenfix.eu/>) for regeneration and calibration prior use.

2.3. Denaturing electrophoresis

The visualization of the proteins present in the extract and the components of the related complex were evaluated through Sodium Dodecyl Sulfate-Polyacrylamide Gel Electrophoresis (SDS-PAGE), with 10% (w/v) separating polyacrylamide/urea gels and 4% (w/v) stacking gels (Fey et al., 2008). The samples were denatured with Rotiload (Roth), boiled for 5 min, and centrifuged before loading. After the electrophoretic separation the gels were stained overnight with Coomassie Brilliant Blue G250 and destained prior visualization.

2.4. Thermal shift assays

The thermal shift assay *in vitro* was then performed on the protein extract which was subjected to a discontinuous temperature gradient in the range between 40 and 100°C by gaps of 10°C. For each of the 7 resulting conditions, triplicates of 80 μL of the extract were tested by incubating them under the tested temperature for 20 min. The same procedure was followed for the experiments at different temperatures but using different pH and salts concentrations (see details in the paragraphs below). After incubation the samples were immediately subjected to denaturation and SDS-PAGE run. Eventually, the theoretical melting temperature (T_{m}), based on the primary sequence, was determined *in silico* by using the software online platform DeepSTABp (<https://csb-deepstabp.bio.rptu.de/>; Jung et al., 2023). A growth temperature range between 20 and 40°C and a cell environment were used as parameters for the calculations.

2.5. Salt concentration assays

Effect under different salt concentrations was evaluated on triplicates of the protein extract in GB buffer under a final concentration of CaCl_2 equivalent to 0 mM, 10 mM (standard condition), 20 mM, and 40 mM. Experiments were carried out on 80 μL of extract under the temperature gradient described in the above paragraph.

2.6. pH Assays

Effect under different pHs was evaluated on triplicates of protein extracts obtained in different buffers depending on the pH tested. In the

experiments by SEC, the pH range 5.0–7.0 was tested, while for SDS-PAGE experiments, the pH range 4.0–8.0 was assessed. Tests at pH 4.0 and 5.0 were performed using Acetate buffer (50 mM CH_3COONa ; 10 mM $\text{MgCl}_2 \cdot 6 \text{H}_2\text{O}$; 10 mM $\text{CaCl}_2 \cdot 2 \text{H}_2\text{O}$); tests at pH 5.5, 6.0 and 6.5 were performed using GB (50 mM MES; 10 mM $\text{MgCl}_2 \cdot 6 \text{H}_2\text{O}$; 10 mM $\text{CaCl}_2 \cdot 2 \text{H}_2\text{O}$), tests at pH 7.0 and 8.0 were performed using Tris-HCl buffer (50 mM Tris, 10 mM $\text{MgCl}_2 \cdot 6 \text{H}_2\text{O}$; 10 mM $\text{CaCl}_2 \cdot 2 \text{H}_2\text{O}$).

2.7. High-resolution ESI-MS and MS/MS analysis

The total crude extract, in triplicate, and the SEC fraction of the main peak (11 mL elution volume) were used for Mass Spectrometry (MS) analysis. Briefly, samples were submitted to in-solution digestion using trypsin (Pierce™ Trypsin Protease, MS Grade – Thermo-Fisher Scientific, Waltham, MA, USA) in enzyme/proteins ratio of 1/50 (w/w). Tryptic peptides extracts were subjected to the desalting procedure using OMIX C18 100 μL pipette tips (Agilent Technologies, Santa Clara, CA, USA) according to the instructions. Peptides were lyophilized and resuspended in aqueous solvent A, 0.1% formic acid (FA) for nano-RP-HPLC-high resolution ESI-MS and MS/MS analysis using an Ultimate 3000 Nano System HPLC (Dionex - Thermo-Fisher Scientific) coupled with a LTQ Orbitrap Elite (Thermo-Fisher Scientific). The Easy Spray reverse-phase nano column (250 mm \times 75 μm inner diameter, Thermo-Fisher Scientific) was a C18 with 2 μm beads. Elution was achieved with aqueous solvent B (0.1% FA, 80% Acetonitrile v/v) in 100 min at a flow rate of 0.3 $\mu\text{L}/\text{min}$ with the following gradient: 0–3 min at 4% B, 3–80 min 4–50% B, 80–90 min 50–80% B, 90–92 min 80–90% B, 92–100 min 90% B. The mass spectrometer was operating at 1.5 kV in the data-dependent acquisition mode, with a capillary temperature of 275 $^\circ\text{C}$ and S-Lens RF level at 68%. Full MS experiments were performed in positive ion mode from 350 to 1600 m/z with resolution 120,000 (at 400 m/z). The 10 most intense ions were subjected to CID fragmentation setting 35% of normalized collision energy for 10 ms, isolation width of 2 m/z and activation q of 0.25. Spectra were acquired by Xcalibur software (v. 3.0, Thermo-Fisher Scientific) and analyzed by Proteome Discoverer (PD) software (v. 2.2, Thermo-Fisher Scientific) with the SEQUEST HT cluster search engine (University of Washington, licensed to Thermo Electron Corporation, San Jose, CA, USA) against the UniProtKB *Nicotiana tabacum* database (894 entries, accessed in July 2023). The precursor peptide mass tolerance was set to 10 ppm, with fragment ion mass tolerance of 0.6 Da. Peptides were filtered for high confidence and a minimum length of 6 amino acids; settings of FDR were 0.01 (strict) and 0.05 (relaxed). Protein abundances were retrieved by PD Label-Free quantification based on the area of unique peptide precursor ions. The mass spectrometry proteomics data have been deposited to the ProteomeXchange Consortium via the PRIDE partner repository (Peréz-Riverol et al., 2022) with the dataset identifier PXD045983.

2.8. Bioinformatic analysis

The primary sequence of the EF1- α has been taken from the Uniprot database (entry P43643) and used in the PeptideCutter software (https://web.expasy.org/peptide_cutter/ - Gasteiger et al., 2005) for predicting possible cleavage sites for specific proteases/molecules.

3. Results

3.1. The soluble fraction extracted from tobacco seeds is primarily composed of a single dominant protein

To profile the primary soluble constituents, we isolated the crude extract from tobacco seeds using mechanical fragmentation. This extract underwent an initial assessment via UV-Vis absorption spectroscopy, revealing a prominent peak at 218 nm as well as a secondary peak at 270–274 nm (Fig. 1). Whereas the first peak suggests the presence of significant amounts of small molecules and/or nucleic acids within the

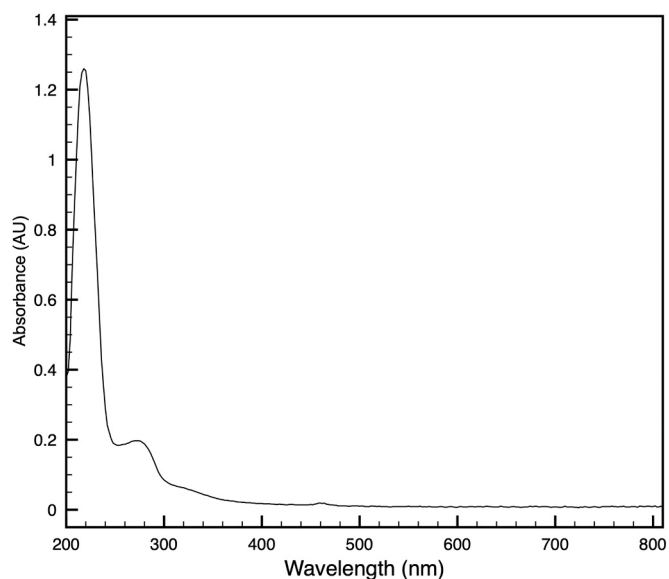


Fig. 1. Analysis of the crude extract solution using absorption spectroscopy. The crude extract solution exhibits a broad absorption band within the UV range, featuring a prominent primary peak at 218 nm accompanied by a less conspicuous secondary peak at 270–274 nm.

extract, the secondary peak can be attributed to the proteinaceous fraction, which in tobacco seeds accounts for 25–30% of their weight (Li et al., 2018; Popova et al., 2018). Accordingly, we further investigated the proteinaceous fraction by profiling the protein composition using denaturing electrophoresis. The analyzed samples exhibited a distinct pattern of bands, with one band at an apparent mass of ~50 kDa standing out prominently in the soluble fractions (Fig. 2). This preliminary characterization therefore indicated that this buffered aqueous solution comprises a combination of proteins and small molecules, underlining the complex nature of the constituents within the tobacco

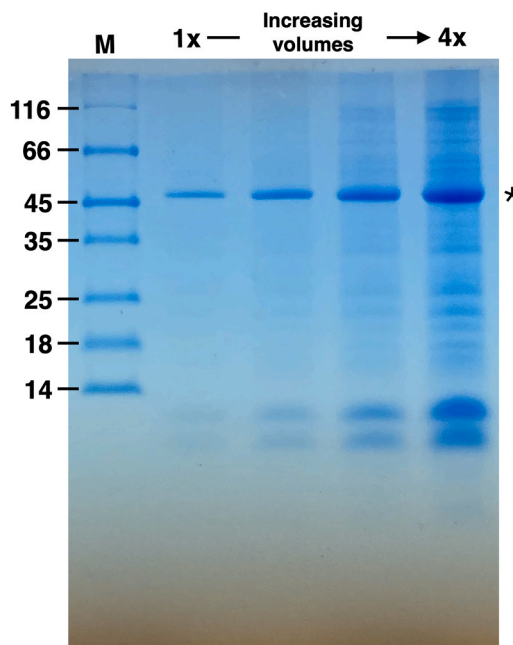


Fig. 2. Denaturing electrophoresis of the crude extract solution. Lanes labeled from 1x to 4x represent varying amounts of loaded crude extract solution (soluble fraction), ranging from one to four times the standard amount. With M is indicated the molecular marker. The asterisk indicates the main protein constituent characteristic of the sample.

seed extract.

3.2. In the extracted soluble fraction, the singular dominant protein exists as a dimer or trimer

Next, the soluble fraction underwent Size Exclusion Chromatography (SEC) with a dual objective: firstly, to determine the oligomeric state of the primary protein component, and, secondly, to assess the presence of other proteins as well as small molecules in the sample. Upon SEC, the sample revealed multiple peaks, with a prominent and distinct one appearing at an elution volume of ~ 11 mL. This dominant peak exhibited an apparent molecular mass of ~ 129.5 kDa, estimated through comparison with a molecular marker (Fig. 3). Furthermore, a group of final peaks with high absorbance was observed at volumes beyond 20 mL, indicating the substantial presence of a small molecules fraction within the crude extract. To rule out the possibility of this final component being a degradation product of the main protein, we subjected a sample from the same stock to a washing process using a 10-kDa-cutoff concentrator. After incubation to allow potential degradation, the sample was then reprocessed using the same method and the aforementioned component at high-elution volumes consistently vanished, confirming that this fraction is not linked to sample degradation events (Fig. 3). Through a comparison between the mass identified by SDS-PAGE (~ 50 kDa) and the one estimated from a regression curve on the SEC column using a molecular marker (129.5 kDa), an oligomerization index of ~ 2.6 has been assigned. This suggests that, *in vivo*, the protein might exist in a dimeric or trimeric form. Subsequently, the extracted protein pools obtained from both the crude extract and the SEC were subjected to MS analysis, finally identifying the main component as the Elongation Factor 1-alpha (EF1- α – Uniprot entry

P43643; Table 1).

Table 1 reports the proteins identified by High-Resolution MS/MS in the crude extract with molecular weight ranging from 73.7 to 11.4 kDa. Among them, EF1- α , Malate dehydrogenase, cytosolic Glyceraldehyde-3-phosphate dehydrogenase, 2-alkenal reductase (NADP(+)-dependent), and Uridine 5'-monophosphate synthase were found enriched in the SEC fraction. Of those, EF1- α was found not only to be the most abundant but also carrying a mass (49.3 kDa) which coincides with the apparent mass of the main band observed in SDS-PAGE.

3.3. The pH selectively affects the solubility of EF1- α

As seeds undergo dehydration in preparation for dormancy, the residual water content diminishes, resulting in a heightened concentration of solutes and, consequently, in a pH reduction (Leprince et al., 2017; Nagel et al., 2015). This change in pH is a contributing factor in sustaining dormancy. As such, pH is anticipated to influence the shift from dormancy to germination, as the pH levels rise alongside decreasing saturation levels. This shift positively impacts protein solubility, potentially contributing to the germination process by allowing the reserves' mobilization. To test this hypothesis, the characterized fraction was subjected to extractions under different pH conditions within the range of 4.0–8.0. As anticipated, at changes toward higher pH values, the extraction of the dominant protein occurred more efficiently, whereas the other proteins in the background also increased but in a much lower extent (Fig. 4). This distinct effect, which selectively enhances the solubilization of the target protein while leaving the rest almost unchanged, allows us to rule out the possibility that the observed effects are merely due to a generic pH-related action. Experiments on the same extracts resolved by SEC confirmed the results observed with denaturing electrophoresis and showed a positive linearity between the increase in pH and the protein solubility (Fig. 4).

3.4. The protein EF1- α senses temperature fluctuations

While pH can serve as an indirect internal signal by reflecting the hydration status of seeds and consequently influencing the transition from dormancy to germination, temperature functions as a direct external trigger. Temperature can directly impact target proteins, especially protein reserves, possibly influencing their solubility (Le Sueur et al., 2022; Peričin et al., 2008). Considering these factors, our next analytical step assessed the protein solubility in response to temperature, testing physiological temperatures and beyond. As anticipated, the rise in temperature generally leads to an increase in solubility. However, as depicted in Fig. 5, this increase did not follow a linear pattern. Moreover, upon incubation at a given temperature, the effect on solubility is also associated with a temperature-dependent degradation pattern (Fig. 5). Increasing temperatures led to the appearance of a secondary band at a molecular weight lower than 40 kDa. This secondary band eventually decreased until its complete disappearance at temperatures above 60°C (Fig. 5, from lane 2–5). Additionally, the concomitant appearance of a second degradation band above 35 kDa was observed (Fig. 5, from lane 5). This phenomenon might likely result from the selective hydroxylamine activity known to be present in seeds during germination (Osuna et al., 2015). Among several others possible cleaving molecules and proteases candidates, PeptideCutter (https://web.expasy.org/peptide_cutter/) predicts hydroxylamine activity at positions 343 and 384 of the amino acid sequence leading to theoretical fragments of approximately 42 kDa and 38 kDa, respectively. This would explain the presence of both these fragments in the SDS-PAGE. Although further investigations are needed, considering its reproducibility, this cleavage could be involved with signaling mechanisms allowing to detect and respond to temperature changes that occur above the optimal range. Beyond 50°C, solubility increases and degradation pattern changes, reaching its peak around 90°C (Fig. 5, lane 8) and collapsing at 100°C (Fig. 5a, lane 9). This behavior, occurring outside

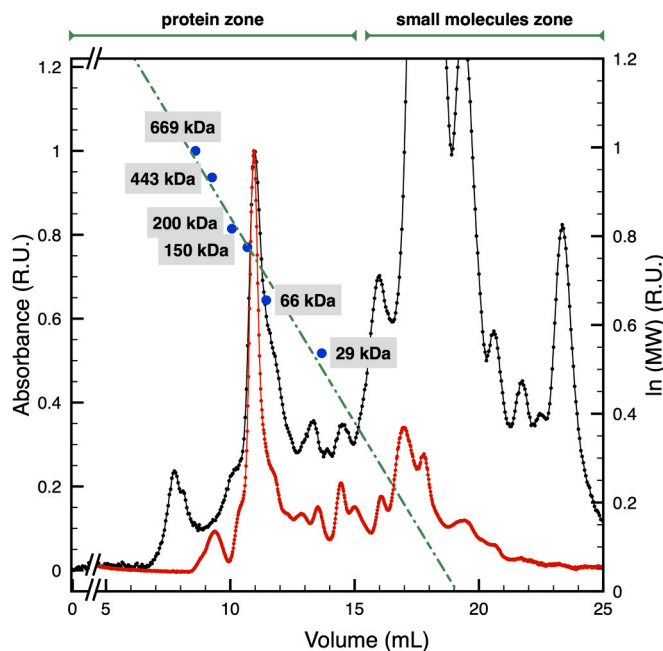


Fig. 3. Size exclusion chromatography of the crude extract solution. In the chromatogram (black curve) obtained from size exclusion chromatography of the crude extract solution, distinct peaks are observed. The peaks with high apparent molecular weights primarily represent proteins (protein zone), while the remaining peaks with low apparent molecular weights correspond to secondary products (small molecules zone). After concentration and subsequent injection, sample degradation was evaluated, yielding the red curve. A molecular marker (blue dots) was employed to estimate the mass of the primary protein component considering its elution volume at 11 mL. Utilizing the resulting regression curve (green dot-dashed line), an apparent mass of 129.5 kDa was determined.

Table 1 - MS analysis of the main protein components in the characterized samples. The table shows the proteins identified by High-Resolution MS/MS listed in order of decreasing abundance as found in the main soluble extract. The molecular weight of the entries ranges between 73.7 and 11.4 kDa. In light grey are indicated the entries that were found to be enriched in the main SEC fraction.

Uniprot ID	Description	MW [kDa]	*PSMs	*Protein Unique Peptides	Replicates Abundances [Average]
P43643	Elongation factor 1-alpha	49.3	36	11	6,64E+07
Q9FSF0	Malate dehydrogenase	35.4	26	11	4,21E+07
Q42962	Phosphoglycerate kinase, cytosolic	42.3	49	14	4,05E+07
P09094	Glyceraldehyde-3-phosphate dehydrogenase, cytosolic (Fragment)	35.5	25	12	2,81E+07
Q9SLN8	2-alkenal reductase (NADP(+)-dependent)	38.1	20	7	2,46E+07
P29449	Thioredoxin H-type 1	13.9	15	6	2,36E+07
Q03461	Non-specific lipid-transfer protein 2	11.4	4	2	1,91E+07
Q9FXS3	Probable phospholipid hydroperoxide glutathione peroxidase	18.8	9	5	1,74E+07
Q56E62	Nucleoside diphosphate kinase 1	16.3	16	6	1,41E+07
Q9XG77	Proteasome subunit alpha type-6	27.3	16	10	1,24E+07
P36182	Heat shock protein 82 (Fragment)	58	19	7	1,21E+07
P69040	Eukaryotic translation initiation factor 5A-1	17.4	3	2	7,71E+06
O82797	Proliferating cell nuclear antigen	29.3	11	6	6,16E+06
P50218	Isocitrate dehydrogenase [NADP]	46.7	8	6	5,39E+06
P68173	Adenosylhomocysteinase	53.1	11	7	4,65E+06
P52885	GTP-binding protein SAR1	22.9	9	3	3,94E+06
Q03685	Luminal-binding protein 5	73.7	61	3	3,55E+06
P93395	Proteasome subunit beta type-6	25.2	7	3	3,34E+06
Q9XHL7	Translationally-controlled tumor protein homolog	18.7	5	3	3,15E+06
Q42942	Uridine 5'-monophosphate synthase (Fragment)	49.7	8	4	2,56E+06
P93342	14-3-3-like protein A	28.6	13	3	2,21E+06
P35494	2,3-bisphosphoglycerate-independent phosphoglycerate mutase	61	4	3	1,60E+06
P40691	Auxin-induced protein PCNT115	33.8	3	3	1,12E+06
Q42946	Oxygen-dependent coproporphyrinogen-III oxidase, chloroplastic	44.9	4	2	9,67E+05
O49995	14-3-3-like protein B	28.8	11	2	5,11E+05

*PSMs: peptide spectrum matches
*Protein Unique Peptides: the total number of distinct peptide sequences unique to the protein.

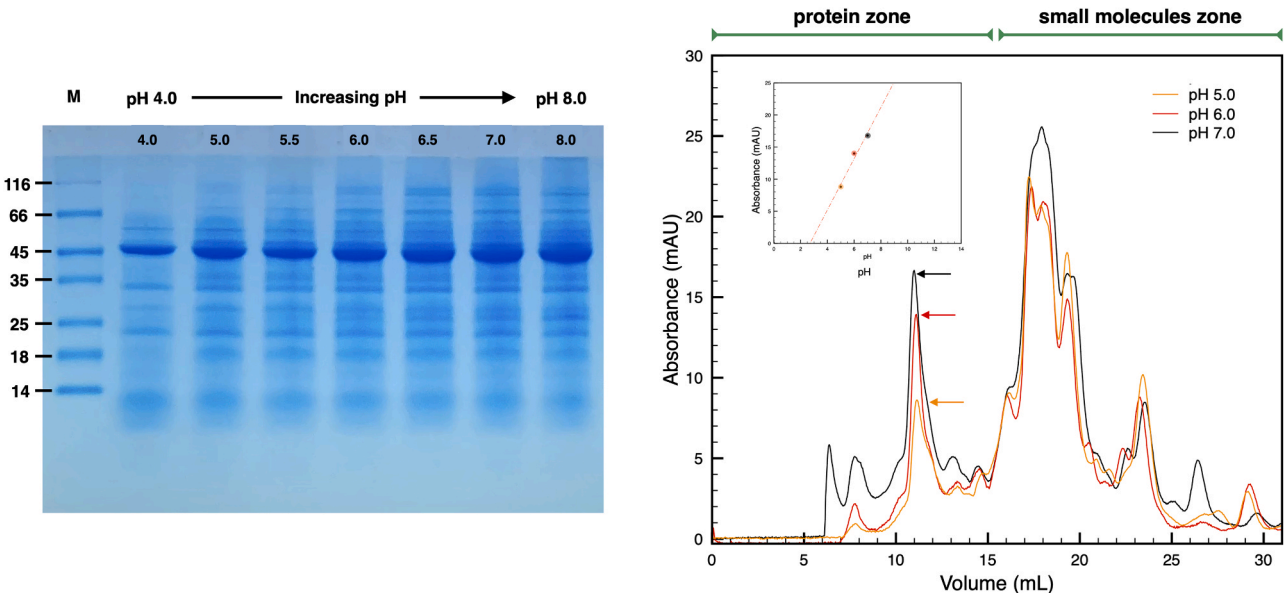


Fig. 4. Effect of pH variation on the crude extract solution. In (A), the gel lanes, marked from pH 4 to pH 8, depict the composition of samples at different pH levels. Notably, as the pH rises, the intensity of the main band also increases, revealing a distinct pH-dependent pattern. With M is indicated the molecular marker. In (B), an increase in pH directly correlates with an increase in the primary constituent of the crude extract when analyzed by SEC, as shown by the increase of the main peak at ~11 mL. This observation reinforces the findings presented in Fig. 4. The three arrows in the graph indicate a clear positive correlation between pH levels and absorbance (indicative of protein quantity). In the inset, a pH versus absorbance plot for the three tested pH conditions is showcased, corresponding to the peaks indicated by the arrows. Additionally, a regression curve (depicted by a red dash-dotted line) is included for reference.

the physiological range, might be related to the protein's structural properties playing a role on solubility at physiological temperatures. When comparing the intensity of the primary band and the heavier degradation band at different temperatures, it is evident that they both exhibit a plateau at lower temperatures. Subsequently, the intensity of the primary band increases while that of the degradation decreases, particularly between 50°C and 60°C. Eventually, the theoretical melting

temperature (T_m) for EF1- α has been calculated. At temperatures within the physiological growth range of 25–30°C, the T_m exhibited values of 51.4 and 53.4°C, respectively. These values fall within the range of temperatures where effective variations in the bands are observed.

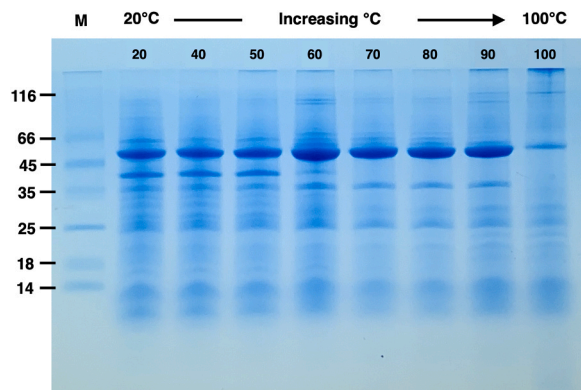


Fig. 5. Effect of Temperature variation on the crude extract solution. In the gel, the lanes, labeled from 20°C to 100°C, illustrate the composition of samples exposed to different temperatures. With increasing temperatures, the intensity of the primary band rises, revealing a discernible temperature-dependent pattern. This trend persists until 90°C. Upon incubation, in the first lanes, two degradation bands appear to be associated with the main protein. The heaviest band vanishes at temperatures exceeding 60°C while the other persists with a slight increase in intensity until 90°C. These bands are likely representing a degradation product of the main band. The lane M indicates the molecular marker.

3.5. The protein EF1- α undergoes degradation prompted by the presence of Ca^{2+}

Given the significance of Ca^{2+} in modulation and signaling, and in order to delve deeper into the impact of chemical-physical factors on protein solubility, we conducted experiments to observe the protein's response at increasing concentrations of this cation. Extraction experiments were conducted at CaCl_2 concentrations of 0, 10, 20, and 40 mM. Similarly to what observed with the temperatures experiments (Fig. 5), concentrations of Ca^{2+} above 20 mM were also found to be correlated with the appearance of the degradation bands (Fig. 6). The intensity of the heaviest band shows a progressive rise with higher cation concentrations (Fig. 6). Notably, the behavior at 20 mM cation concentration, with an apparent decrease in the main band, coincides with a substantial surge in the secondary band. This hints at an overall increase in the total protein where a portion underwent cleavage, potentially indicating a

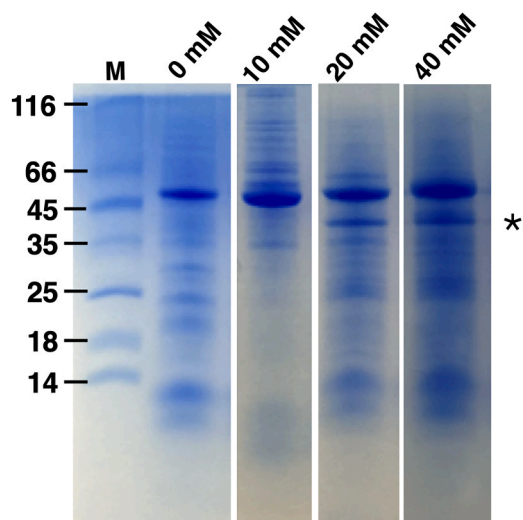


Fig. 6. Impact of Ca^{2+} concentration on the crude extract solution. As the concentration of Ca^{2+} increases from 0 to 40 mM, starting from 10 mM (with a faint band) onwards appears a degradation band (marked with an asterisk) with increases its intensity at high concentrations of Ca^{2+} .

regulatory mechanism at play.

4. Conclusions

Dormancy and germination are essential processes in the plant life cycle and rely on the correct assessment of seed status in relation to the surrounding environment (Footitt et al., 2013; Weitbrecht et al., 2011). Hence, these vital processes depend on either indirect signals from effectors or direct ones from the inherent capability of the target protein itself (Dorone et al., 2021; Jin et al., 2018). The latter ability encompasses sensing internal factors like pH, osmotic potential, and water potential, as well as external factors such as temperature and photons (Ma et al., 2019; Park et al., 2018; Wilkinson and Strader, 2020). In this context, direct sensing holds significance due to its ability to provide swift responses independent of upstream processes. This attribute becomes particularly crucial during the initial stages of processes where activation begins from the very outset, triggering prompt "sparking" events. In the case of seeds, these considerations are especially pertinent for vital processes such as the accumulation of reserves in preparation to dormancy or their mobilization during germination (Dorone et al., 2021; Field et al., 2023; Piskurewicz et al., 2023). In this study, our primary focus has been to elucidate the distinct effects of chemical and physical factors on dormancy/germination, with a particular emphasis on the most abundant protein, the EF1- α . Known for its pivotal role in protein expression and ribosome regulation through its GTPase activity, the EF1- α was here identified as the predominant protein in tobacco seeds, providing supporting evidence for its role as a reserve protein. The protein EF1- α has been initially isolated and then subjected to a fundamental biochemical characterization, including its MS identification (Figs. 1 to 3 and Table 1). Following that, an investigation into the solubility of EF1- α was carried out under different pH values, temperatures, and salt concentrations (Figs. 4–6). In general, these chemical-physical factors hold significant importance within the framework of direct sensing mechanisms. They not only directly influence the protein target but also undergo considerable variations during the shift from seed differentiation to dormancy and subsequently from dormancy to germination. Here, analyses of these factors on the EF1- α protein revealed a distinct alteration in its solubility and stability compared to the other proteins within the extract. The selective effect observed here could be linked to direct sensing processes during which the alteration induced on the protein may stand as the primary discriminator between dormancy, characterized by protein insolubility, and germination, characterized by the increased solubility of reserves. Of outmost significance, the three variables (pH, temperature, and Ca^{2+} concentration) examined for their effectiveness in affecting EF1- α solubility operated within physiological ranges, leading to consistency between observations and physiological implications. Notably, these findings align with the established sensitivities of EF1- α observed in various species and metabolic contexts (Ransom-Hodgkins et al., 2000; Fu et al., 2012; Kuang et al., 2019; Xu et al., 2023).

The distinct impact caused by pH variations within the physiological range indicated that, when the pH shifts toward low values, the solubility of EF1- α diminishes (Fig. 4). This phenomenon is anticipated to occur *in vivo* during preparation to dormancy, where dehydration processes coincide with an increased solute concentration and a subsequent decrease in pH. A comparable rationale can be applied to the converse scenario of seed hydration and germination. Consequently, increased solute concentrations during seed dehydration serve as a clear indicator toward dormancy, complementing the negative variations in pH associated with these changes (Fig. 6). This mechanism encompasses an array of solutes, including salts and proteins. This is also valid for a specific regulatory cation like Ca^{2+} , with roles in numerous regulatory processes. In a state of dehydration, high solutes concentration and low pH, are associated to a significant increase in $[\text{Ca}^{2+}]$ reaching values far beyond its typical physiological levels. Therefore, an anomalous behavior is anticipated as a result of the interplay between the seed's

dehydration requirements (associated with high concentrations of Ca^{2+}) and the regular signaling dynamics mediated by Ca^{2+} , where the cation is typically present at low concentrations ($< 2 \text{ mM}$), exerting its effects through temporary spikes in concentration ($10\text{--}20 \text{ mM}$) that serve as signaling functions. Experiments involving Ca^{2+} validated the predicted anomalous behavior, where the solubility of EF1- α arises from the interplay of two opposing phenomena (Fig. 6). The first is an increased solubility linked to a rise in calcium concentration within lower and cellular ranges ($0\text{--}10 \text{ mM}$), which is expected to occur during rehydration and germination scenarios. Within this range, calcium levels align with the typical signaling values ($1\text{--}10 \text{ mM}$). This effect can lead to a modulation of the protein concentration in solution, possibly through conformational changes, aligning with conditions in which, as indicated by the pH tests, the pH values tend to increase as expected with rehydration and subsequent germination (Fig. 4).

The second behavior manifests when Ca^{2+} concentrations exceed 10 mM , creating a context where the cation levels significantly surpass the standard intracellular concentrations. This scenario is pertinent to circumstances connected with dehydration and dormancy. Remarkably, under these conditions, EF1- α also undergoes partial cleavage, a characteristic previously documented for this protein but in different metabolic contexts (Ransom-Hodgkins et al., 2000) and that might be the result of a selective hydroxylamine activity, which is important during germination (Osuna et al., 2015) and for which the predicted cleavage fragment agrees with the findings here reported.

The mechanism by which the seed is able to distinguish between the first and the second scenario could be attributed to a selective EF1- α cleavage enhanced by $[\text{Ca}^{2+}]$, providing a discriminant mechanism by which this protein could serve as a key target in signal transduction pathways (Ransom-Hodgkins et al., 2000) to distinguish between dormancy and germination. Regarding the second behavior, there might appear to be a paradox, as elevated concentrations of Ca^{2+} are usually linked to lower pH, which is, in turn, associated with reduced protein solubility rather than the contrary. However, it's important to consider that during this particular circumstance, the pH is indeed low (reflecting dormancy). In these conditions, the presence of protein in the solution is constrained by the pH but linked to the distinctive degradation band that acts as a discriminant. This once again confirms a pure signal behavior in this scenario.

Equally important is the role of temperature. The lack of a linear trend within the temperature range just above the upper limit of the physiological interval as well as the appearance of two protein bands related to the main one in the same interval, represents a non-random signal (Fig. 5). This signal, processed by the seed through the protein, could serve as an indicator of unfavorable external conditions, possibly linked to occurring environmental conditions associated to high temperatures and dryness.

The current study has highlighted the significance of EF1- α in conveying environmental cues to the seed via alterations in its solubility and stability, which result from the interplay of solute concentration, pH, and temperature. In real-world scenarios, these effects are anticipated to interact collectively, possibly involving various other factors. It's likely that not only EF1- α but also other proteins utilize similar property changes as responses to shifts in the internal or external environment. Significantly, the EF1- α presence in the seed is consistent with similar studies in maize, where this factor has been used as an indicator of the protein reserves' quality in the endosperm on the base of its regulatory role in cytoskeletal organization (Lopez-Valenzuela et al., 2004; Sun et al., 1997). The high amount found here suggests a direct involvement of EF1- α as a reserve protein, confirming again its multifaceted role within multiple cellular processes.

Additional research on this system will be crucial in unraveling the precise mechanisms underlying these effects. A deeper comprehension of these processes will yield valuable insights into the molecular mechanisms occurring during the transition from seed dormancy to germination.

CRediT authorship contribution statement

Emma Cocco: Writing – review & editing, Writing – original draft, Visualization, Methodology, Investigation, Formal analysis, Conceptualization. **Giulia Guadalupi:** Writing – review & editing, Writing – original draft, Visualization, Methodology, Investigation, Formal analysis. **Domenica Farci:** Writing – review & editing, Writing – original draft, Visualization, Validation, Methodology, Investigation, Formal analysis, Data curation, Conceptualization. **Andrea Maxia:** Writing – review & editing, Writing – original draft, Validation, Methodology. **Barbara Manconi:** Writing – review & editing, Writing – original draft, Visualization, Validation, Methodology, Investigation. **Dario Piano:** Writing – review & editing, Writing – original draft, Visualization, Validation, Supervision, Resources, Project administration, Methodology, Investigation, Funding acquisition, Formal analysis, Data curation, Conceptualization.

Declaration of Competing Interest

The authors declare that they have no known competing financial interests or personal relationships that could have appeared to influence the work reported in this paper.

Data availability

Data will be made available on request.

Acknowledgments

We acknowledge the CeSAR (Centro Servizi d'Ateneo per la Ricerca) of the University of Cagliari (Italy) for the HR-MS/MS experiments performed with the HPLC-LTQ Orbitrap Elite

References

- A. Ali, J.M. Pardo, D.J. Yun, Desensitization of ABA-Signaling: the swing from activation to degradation, *Front. Plant Sci.* 11 (2020) 379, <https://doi.org/10.3389/fpls.2020.00379>.
- Z. Adam, Protein stability and degradation in chloroplasts, *Plant Mol. Biol.* 32 (5) (1996) 773–783, <https://doi.org/10.1007/BF00020476>.
- M. Agacka-Moldoch, M.A. Rehman Arif, U. Lohwasser, T. Doroszewska, R.S. Lewis, A. Börner, QTL analysis of seed germination traits in tobacco (*Nicotiana tabacum* L.), *J. Appl. Genet.* 62 (3) (2021) 441–444, <https://doi.org/10.1007/s13353-021-00623-6>.
- R. Antoni, L. Rodriguez, M. Gonzalez-Guzman, G.A. Pizzio, P.L. Rodriguez, News on ABA transport, protein degradation, and ABFs/WRKYs in ABA signaling, *Curr. Opin. Plant Biol.* 14 (5) (2011) 547–553, <https://doi.org/10.1016/j.pbi.2011.06.004>.
- E. Cocco, D. Farci, P. Haniewicz, W.P. Schröder, A. Maxia, D. Piano, The influence of blue and red light on seed development and dormancy in *Nicotiana tabacum* L., *Seeds* 1 (3) (2022) 152–163.
- Y. Dorone, S. Boeynaems, E. Flores, et al., A prion-like protein regulator of seed germination undergoes hydration-dependent phase separation, *Cell* 184 (16) (2021) 4284–4298, <https://doi.org/10.1016/j.cell.2021.06.009>.
- F. Faden, S. Mielke, N. Dissmeyer, Modulating protein stability to switch toxic protein function on and off in living cells, *Plant Physiol.* 179 (3) (2019) 929–942, <https://doi.org/10.1104/pp.18.01215>.
- D. Farci, P. Haniewicz, E. Cocco, A. De Agostini, P. Cortis, M. Kusaka, M.C. Loi, D. Piano, The impact of fruit etiolation on quality of seeds in tobacco, *Front. Plant Sci.* 11 (2020) 563971, <https://doi.org/10.3389/fpls.2020.563971>.
- H. Fey, D. Piano, R. Horn, D. Fischer, M. Schmidt, S. Ruf, W.P. Schröder, R. Bock, C. Büchel, Isolation of highly active photosystem II core complexes with a His-tagged Cyt b559 subunit from transplastomic tobacco plants, *Biochim. Et. Biophys. Acta* 1777 (12) (2008) 1501–1509, <https://doi.org/10.1016/j.bbabo.2008.09.012>.
- S. Field, G.J. Jang, C. Dean, L.C. Strader, S.Y. Rhee, Plants use molecular mechanisms mediated by biomolecular condensates to integrate environmental cues with development, *Plant Cell* 35 (9) (2023) 3173–3186, <https://doi.org/10.1093/plcell/koad062>.
- S. Footitt, Z. Huang, H.A. Clay, A. Mead, W.E. Finch-Savage, Temperature, light and nitrate sensing coordinate Arabidopsis seed dormancy cycling, resulting in winter and summer annual phenotypes, *Plant J.: Cell Mol. Biol.* 74 (6) (2013) 1003–1015, <https://doi.org/10.1111/tpj.12186>.
- J. Fu, I. Momčilović, P.V.V. Prasad, Roles of protein synthesis elongation factor EF-Tu in heat tolerance in plants, *J. Bot.* (2012) 1–8, <https://doi.org/10.1155/2012/835836>.
- Gasteiger E., Hoogland C., Gattiker A., Duvaud S., Wilkins M.R., Appel R.D., Bairoch A. 2005. Protein identification and analysis tools on the ExPASy server. In: Walker, J.M.

- (eds) The Proteomics Protocols Handbook. Springer Protocols Handbooks. Humana Press. <https://doi.org/10.1385/1-59259-890-0:571>.
- P. Haniewicz, D. Floris, D. Farci, J. Kirkpatrick, M.C. Loi, C. Büchel, M. Bachtler, D. Piano, Isolation of plant photosystem II complexes by fractional solubilization, *Front. Plant Sci.* 6 (2015) 1100, <https://doi.org/10.3389/fpls.2015.01100>.
- T.J. Holman, P.D. Jones, L. Russell, et al., The N-end rule pathway promotes seed germination and establishment through removal of ABA sensitivity in *Arabidopsis*, *Proc. Natl. Acad. Sci. USA* 106 (11) (2009) 4549–4554, <https://doi.org/10.1073/pnas.0810280106>.
- D. Jin, M. Wu, B. Li, et al., The COP9 Signalosome regulates seed germination by facilitating protein degradation of RGL2 and ABI5, *PLoS Genet* 14 (2) (2018) e1007237, <https://doi.org/10.1371/journal.pgen.1007237>.
- F. Jung, K. Frey, D. Zimmer, T. Mühlhaus, DeepSTABp: a deep learning approach for the prediction of thermal protein stability, *Int. J. Mol. Sci.* 24 (8) (2023) 7444, <https://doi.org/10.3390/ijms24087444>.
- P. Jurkiewicz, H. Batoko, Protein degradation mechanisms modulate abscisic acid signaling and responses during abiotic stress, *Plant Sci.: Int. J. Exp. Plant Biol.* 267 (2018) 48–54, <https://doi.org/10.1016/j.plantsci.2017.10.017>.
- L. Kuang, Q. Shen, L. Wu, J. Yu, L. Fu, D. Wu, G. Zhang, Identification of microRNAs responding to salt stress in barley by high-throughput sequencing and degradome analysis, *Environ. Exp. Bot.* 160 (2019) 59–70, <https://doi.org/10.1016/j.envexpbot.2019.01.006>.
- C. Le Sueur, H.M. Hammarén, S. Sridharan, M.M. Savitski, Thermal proteome profiling: insights into protein modifications, associations, and functions, *Curr. Opin. Chem. Biol.* 71 (2022) 102225, <https://doi.org/10.1016/j.cbpa.2022.102225>.
- O. Leprince, A. Pellizzaro, S. Berriri, J. Buitink, Late seed maturation: drying without dying, *J. Exp. Bot.* 68(4), 827–841 (2017), <https://doi.org/10.1093/jxb/erw363>.
- Z. Li, F. Li, G. Guo, Y. Gao, W. Ma, R. Pan, Y. Guan, Jin Hu, Evaluation of seed quality based on changes of internal substances during tobacco seed (*Nicotiana tabacum* L.) development, *Plant Growth Regul.* 86 (2018) 389–399, <https://doi.org/10.1007/s10725-018-0437-x>.
- Z. Li, J. Zhang, Y. Liu, J. Zhao, J. Fu, X. Ren, G. Wang, J. Wang, Exogenous auxin regulates multi-metabolic network and embryo development, controlling seed secondary dormancy and germination in *Nicotiana tabacum* L., *BMC Plant Biol.* 16 (2016) 41, <https://doi.org/10.1186/s12870-016-0724-5>.
- Q. Ling, W. Broad, R. Trösch, M. Töpel, T. Demiral Sert, P. Lymperopoulos, A. Baldwin, R.P. Jarvis, Ubiquitin-dependent chloroplast-associated protein degradation in plants, *Science* 363 (6429) (2019) eaav4467, <https://doi.org/10.1126/science.aav4467>.
- J.A. Lopez-Valenzuela, B.C. Gibbon, D.R. Holding, B.A. Larkins, Cytoskeletal proteins are coordinately increased in maize genotypes with high levels of eEF1A, *Plant Physiol.* 135 (3) (2004) 1784–1797, <https://doi.org/10.1104/pp.104.042259>.
- W. Ma, X. Guan, J. Li, et al., Mitochondrial small heat shock protein mediates seed germination via thermal sensing, *Proc. Natl. Acad. Sci. USA* 116 (10) (2019) 4716–4721, <https://doi.org/10.1073/pnas.1815790116>.
- M. Nagel, I. Kranner, K. Neumann, H. Rolletschek, C.E. Seal, L. Colville, B. Fernández-Marín, A. Börner, Genome-wide association mapping and biochemical markers reveal that seed ageing and longevity are intricately affected by genetic background and developmental and environmental conditions in barley, *Plant, Cell Environ.* 38 (6) (2015) 1011–1022, <https://doi.org/10.1111/pce.12474>.
- D. Osuna, P. Prieto, M. Aguilar, Control of seed germination and plant development by carbon and nitrogen availability, *Nov 18, Front Plant Sci.* 6 (2015) 1023, <https://doi.org/10.3389/fpls.2015.01023>.
- E. Park, Y. Kim, G. Choi, Phytochrome B requires PIF degradation and sequestration to induce light responses across a wide range of light conditions, *Plant Cell* 30 (6) (2018) 1277–1292, <https://doi.org/10.1105/tpc.17.00913>.
- Y. Perez-Riverol, J. Bai, C. Bandla, et al., The PRIDE database resources in 2022: a hub for mass spectrometry-based proteomics evidences, *Nucleic Acids Res.* 7 50 (D1) (2022) D543–D552, <https://doi.org/10.1093/nar/gkab1038>.
- D. Peričin, L. Radulović, S. Trivić, E. Dimić, Evaluation of solubility of pumpkin seed globulins by response surface method, *J. Food Eng.* 84 (4) (2008) 591–594, <https://doi.org/10.1016/j.jfoodeng.2007.07.002>.
- U. Piskurewicz, M. Sentandreu, M. Iwasaki, G. Glauser, L. Lopez-Molina, The Arabidopsis endosperm is a temperature-sensing tissue that implements seed thermoinhibition through phyB, *Nat. Commun.* 14 (2023) 1202, <https://doi.org/10.1038/s41467-023-36903-4>.
- V. Popova, Z. Petkova, T. Ivanova, M. Stoyanova, L. Lazarov, A. Stoyanova, et al., Biologically active components in seeds of three nicotiana species, *Ind. Crops Prod.* 117 (2018) 375–381, <https://doi.org/10.1016/j.indcrop.2018.03.020>.
- W.D. Ransom-Hodgkins, I. Brglez, X. Wang, W.F. Boss, Calcium-regulated proteolysis of eEF1A, *Plant Physiol.* 122 (3) (2000) 957–965, <https://doi.org/10.1104/pp.122.3.957>.
- Y. Sun, N. Carneiro, A.M. Clore, G.L. Moro, J.E. Habben, B.A. Larkins, Characterization of maize elongation factor 1A and its relationship to protein quality in the endosperm, *Plant Physiol.* 115 (3) (1997) 1101–1107, <https://doi.org/10.1104/pp.115.3.1101>.
- M.I. Villalobos Solis, S. Poudel, C. Bonnot, H.K. Shrestha, R.L. Hettich, C. Veneault-Fourrey, F. Martin, P.E. Abraham, A viable new strategy for the discovery of peptide proteolytic cleavage products in plant-microbe interactions, *Mol. Plant-Microbe Interact.: MPMI* 33 (10) (2020) 1177–1188, <https://doi.org/10.1094/MPMI-04-20-0082-TA>.
- K. Weitbrecht, K. Müller, G. Leubner-Metzger, First off the mark: early seed germination, *J. Exp. Bot.* 62 (10) (2011) 3289–3309, <https://doi.org/10.1093/jxb/err030>.
- E.G. Wilkinson, L.C. Strader, A prion-based thermosensor in plants, *Mol. Cell* 80 (2) (2020) 181–182, <https://doi.org/10.1016/j.molcel.2020.09.026>.
- L. Xu, L. Zhang, Y. Liu, B. Sod, M. Li, T. Yang, T. Gao, Q. Yang, R. Long, Overexpression of the elongation factor MtEF1A1 promotes salt stress tolerance in *Arabidopsis thaliana* and *Medicago truncatula*, *BMC Plant Biol.* 23 (1) (2023) 138, <https://doi.org/10.1186/s12870-023-04139-5>.
- K. Zientara-Rytter, A. Sirko, To deliver or to degrade - an interplay of the ubiquitin-proteasome system, autophagy and vesicular transport in plants, *FEBS J.* 283 (19) (2016) 3534–3555, <https://doi.org/10.1111/febs.13712>.